Inorg. Chem. **2002**, *41*, 5216–5225

Participation of Co-Ligands in Electronic Transitions of Platinum(II) Diazabutadiene Complexes

Axel Klein,*,† Joris van Slageren,‡ and Stanislav Záliš§

Institut für Anorganische Chemie, Universität Stuttgart, Pfaffenwaldring 55, D-70569 Stuttgart, Germany, Institute of Molecular Chemistry, Universiteit van Amsterdam, Nieuwe Achtergracht 166, NL-1018 WV Amsterdam, The Netherlands, and J. Heyrovský Institute of Physical Chemistry, Academy of Sciences of the Czech Republic, Dolejškova 3, CZ-18 000 Prague 8, Czech Republic

Received February 19, 2002

The low-lying electronic transitions and photochemical reactions of a series of [(ⁱPr-DAB)Pt(R)$_2$] (where the co-ligand R = CH_3, CD_3, adme, neop, neoSi, C≡C^{t}Bu, C≡CPh, Ph, Mes) compounds were studied using both experimental (electronic absorption and resonance Raman spectroscopy) and theoretical (density functional theory, DFT) techniques. The high-lying filled orbitals were revealed to have a significant co-ligand contribution in the case of alkyl complexes, while this contribution is predominant for the complexes with unsaturated co-ligands. Because the electronic transition removes electron density from the σ(Pt–C) bond in the former complexes, it is best described as a metal-to-ligand charge transfer transition (MLCT) with partial sigma-bond-to-ligand charge transfer (SBLCT) character. Because the σ(Pt–C) orbital is not involved in the HOMOs of the latter complexes, the low-lying transitions were characterized as mixed MLCT/L′LCT, where L′LCT stands for ligand-to-ligand charge transfer from the π system of the unsaturated co-ligand to the π^*(ⁱPr-DAB) orbital. The alkyl complexes are photoreactive on visible light irradiation with Pt–C bond homolysis as the primary step. The efficiency of the photoreaction increases with increasing σ donor strength of the alkyl ligand. The absolute quantum yield is quite low. The other complexes are virtually photostable, except when irradiated at relatively high energies.

Introduction

Organoplatinum(II) complexes of the type [(α-diimine)-Pt(R)$_2$] with R = alkyl, alkynyl, or aryl are widely studied.[1−13] One of the main reasons is that these complexes have moderately strong tunable absorption bands in the visible spectrum. Depending on the nature of R, they can show luminescence, even in fluid solution at ambient temperatures,[3,5,7,9,11,12] which makes them attractive for various applications in the molecular photonics field.[14−18] Generally, low-energy electronic absorption bands are ascribed to metal-to-ligand charge transfer (MLCT) absorption

* To whom correspondence should be addressed. E-mail: aklein@iac.uni-stuttgart.de.
† Universität Stuttgart.
‡ Universiteit van Amsterdam.
§ Academy of Sciences of the Czech Republic. E-mail: zalis@jh-inst.cas.cz.

(1) Von Zelewsky, A.; Belser, P.; Hayoz, P.; Dux, R.; Hua, X.; Suckling, A.; Stoeckli-Evans, H. *Coord. Chem. Rev.* **1994**, *132*, 75.
(2) Chaudhury, N.; Puddephatt, R. J. *J. Organomet. Chem.* **1975**, *84*, 105.
(3) Hissler, M.; McGarrah, J. E.; Connick, W. B.; Geiger, D. K.; Cummings, S. D.; Eisenberg, R. *Coord. Chem. Rev.* **2000**, *208*, 115.
(4) Hissler, M.; Connick, W. B.; Geiger, D. K.; McGarrah, J. E.; Lipa, D.; Lachicotte, R. J.; Eisenberg, R. *Inorg. Chem.* **2000**, *39*, 447.
(5) Connick, W. B.; Geiger, D.; Eisenberg, R. *Inorg. Chem.* **1999**, *38*, 3264.
(6) Paw, W.; Cummings, S. D.; Mansour, M. A.; Connick, W. B.; Geiger, D. K.; Eisenberg, R. *Coord. Chem. Rev.* **1998**, *171*, 125.
(7) Connick, W. B.; Miskowski, V. M.; Houlding, V. H.; Gray, H. B. *Inorg. Chem.* **2000**, *39*, 2585.
(8) Ng, Y.-Y.; Che, C.-M.; Peng, S.-M. *New J. Chem.* **1996**, *20*, 781.
(9) Chan, C.-W.; Cheng, L.-K.; Che, C.-M. *Coord. Chem. Rev.* **1994**, *132*, 87.
(10) Whittle, C. E.; Weinstein, J. A.; George, M. W.; Schanze, K. S. *Inorg. Chem.* **2001**, *40*, 4053.
(11) Kaim, W.; Klein, A. *Organometallics* **1995**, *14*, 1176.
(12) Vogler, C.; Schwederski, B.; Klein, A.; Kaim, W. *J. Organomet. Chem.* **1992**, *436*, 367.
(13) Dungey, K. E.; Thompson, B. D.; Kane-Maguire, N. A. P.; Wright, L. L. *Inorg. Chem.* **2000**, *39*, 5192.
(14) Balzani, V.; Credi, A.; Venturi, M. *Coord. Chem. Rev.* **1998**, *171*, 3.
(15) Balzani, V.; Scandola, F. *Supramolecular Photochemistry*; Ellis Horwood: Chichester, U.K., 1991.
(16) Balzani, V.; Juris, A. *Coord. Chem. Rev.* **2001**, *211*, 97.
(17) Scandola, F.; Argazzi, R.; Bignozzi, C. A.; Chiorboli, C.; Indelli, M. T.; Rampi, M. A. Antenna Effects and Photoinduced Electron Transfer in Polynuclear Metal Complexes. In *Supramolecular Chemistry*; de Cola, L., Balzani, V., Eds.; NATO ASI Series C; Kluwer: Dordrecht, The Netherlands, 1992; Vol. 371, p 235.
(18) McGarrah, J. E.; Kim, Y.-J.; Hissler, M.; Eisenberg, R. *Inorg. Chem.* **2001**, *40*, 4510.

10.1021/ic025547o CCC: $22.00
Published on Web 09/10/2002

Scheme 1. Schematic Representation of ^{i}Pr-DAB = *N*,*N*′-Diisopropyl-1,4-diazabutadiene in the Noncoordinating Free Form (Left) and in the Square Planar Platinum(II) Complexes [(^{i}Pr-DAB)Pt(R)$_2$] (Right)

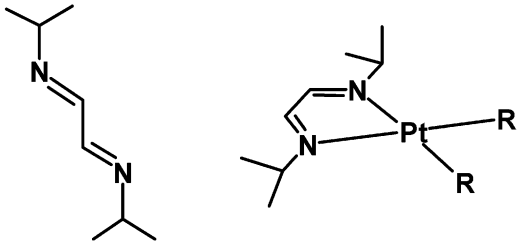

bands. Correspondingly, the lowest excited state is usually assumed to have MLCT character as well. These assignments agree with the pronounced solvatochromism and the extinction coefficients of the absorption bands.

In recent studies on a series of [(COD)Pt(R)$_2$] complexes (COD = 1,5-cyclooctadiene), we have found that the high lying occupied orbitals are not exclusively located on the Pt atom.[19] For R = alkyl, these orbitals show increasing contributions of the R ligand with increasing σ donor strength of that ligand. If R possesses π orbitals, as in the case of R = alkynyl or aryl, it was shown that these form to a large extent the high lying occupied orbitals of the molecule. One consequence of this situation is that the complexes are photoreactive in solution at room temperature. Irradiation leads to the formation of R radicals in the case of alkyl complexes, and to R−R coupling products if R is an alkynyl ligand. The drawback of these systems for applications such as photoinitiators or sources of predefined organic radicals is the fact that the absorption bands occur in the near UV (350−390 nm).

The aim of this paper is therefore twofold. First of all, we were interested in preparing complexes that are photoreactive under visible light irradiation. To this end, we synthesized a series of [(α-diimine)Pt(R)$_2$] complexes with different co-ligands R. As stated previously, the absorption bands of such compounds are located well in the visible range. The other aim was to determine to which extent the R ligands participate in the low lying electronic transitions of these complexes and thus assess the validity of the generally accepted MLCT assignments of the lowest-energy absorption bands. Among the co-ligands included in this study are alkyl groups of varying σ donor strength (CH_3, CD_3, adme = 1-adamantylmethyl, neop = neopentyl = 2,2-dimethyl-1-methyl, neoSi = neosilyl = trimethylsilylmethyl). Furthermore, several complexes with unsaturated co-ligands (C≡C^{t}Bu, C≡CPh, Ph, Mes) were prepared. As the α-diimine ligand, ^{i}Pr-DAB (*N*,*N*′-diisopropyl-1,4-diaza-1,3-butadiene)[20] (see Scheme 1) was used; its simple structure makes both the interpretation of experimental data as well as theoretical calculations easier.[21−23] The electronic structure of the complexes was calculated using density functional theory (DFT) methods, which were also used to determine the nature of the low-energy electronic transitions. Additionally, these transitions were studied by resonance Raman (rR) spectroscopy, this being virtually the only technique that gives direct experimental information about the nature of electronic transitions which are responsible for observed absorption bands. The vibrations which were found in the rR spectra were assigned by comparison with DFT calculations of the molecular vibrations.

Experimental Section

Synthesis. All preparations and manipulations were carried out under an inert atmosphere of argon or nitrogen. All complexes were prepared and examined under protection from intense light. The dimethyl or dimesityl complexes [(R′-DAB)Pt(R)$_2$] (R = CH_3 or Mes) were prepared as previously published for related complexes,[24−26] from [$(CH_3)_2$Pt(μ-SMe_2)Pt$(CH_3)_2$][27] or [$(dmso)_2$Pt$(Mes)_2$][28] and the corresponding R′-DAB ligands.[20] The organoplatinum COD (1,5-cyclooctadiene) or NBD (norbornadiene = bicyclo[2.2.1]hepta-2,5-diene) complexes including the deuterated derivative [(NBD)Pt$(CD_3)_2$] were obtained as previously described for the COD derivatives.[19]

General Procedure for the Synthesis of [(^{i}Pr-DAB)Pt(R)$_2$]. The appropriate starting complexes [(diolefin)Pt(R)$_2$] (diolefin = COD, NBD) (1 equiv, usually 500 mg) and 2 equiv of ^{i}Pr-DAB were suspended in mixtures of 100 mL of diethyl ether and 100 mL of toluene and stirred at the required conditions (see following paragraphs, given as *T* for reaction temperature and time for reaction time). The products for R = Ph, Mes, CH_3, adme, C≡C^{t}Bu, or C≡CPh were obtained by evaporation of the reaction mixtures to dryness, extraction of the residues with CH_2Cl_2, and crystallization from CH_2Cl_2/heptane (1:3) mixtures. The reaction for R = neop or neoSi was driven only to conversions of 50%. The products were isolated by evaporation of the reaction mixtures to dryness and subsequent extraction of the residues with several portions of *n*-pentane. Careful recrystallization from *n*-pentane gave the pure microcrystalline materials.

[(^{i}Pr-DAB)Pt$(CH_3)_2$]. From [(COD)Pt$(CH_3)_2$], T = 343 K, time 20 h. Yield (violet powder): 83%. Anal. Calcd for $C_{10}H_{22}N_2Pt$: C, 32.87; H, 6.07; N, 7.67%. Found: C, 32.88; H, 6.10; N, 7.68%. ^{1}H NMR (CD_2Cl_2) δ (ppm): 1.43 (d, 12 H, ^3J = 6.61 Hz, CH$(CH_3)_2$), 1.45 (s, 6H, $^2J_{Pt-H}$ = 85.05 Hz, PtCH_3), 4.60 (septet, 2H, $CH(CH_3)_2$), 9.02 (s, 2H, $^3J_{Pt-H}$ = 34.8 Hz, H_{imino}).

[(^{i}Pr-DAB)Pt$(CD_3)_2$]. From [(NBD)Pt$(CD_3)_2$], T = 343 K, time 14 h. Yield (violet powder): 87%. ^{1}H NMR (CD_2Cl_2) δ (ppm): 1.43 (d, 12 H, ^3J = 6.61 Hz, CH$(CH_3)_2$), 4.60 (septet, 2H, $CH(CH_3)_2$), 9.02 (s, 2H, $^3J_{Pt-H}$ = 34.8 Hz, H_{imino}), no signal due to Pt−CH_3.

[(^{i}Pr-DAB)Pt(neop)$_2$] (neop = Neopentyl or 2,2-Dimethylpropyl). From [(NBD)Pt(neop)$_2$], T = 333 K, time 120 h. Yield (blue powder): 66% (conversion 50%). Anal. Calcd for $C_{18}H_{38}N_2$Pt: C, 45.27; H, 8.02; N, 5.87%. Found: C, 45.13; H, 8.05; N, 5.84%. ^{1}H NMR (CD_2Cl_2) δ (ppm): 1.00 (s, 18 H, C$(CH_3)_3$), 1.42

(19) Klein, A.; van Slageren, J.; Zalis, S. *J. Organomet. Chem.* **2001**, *620*, 202.
(20) Bock, H.; tom Dieck, H. *Angew. Chem.* **1966**, *78*, 549.
(21) Stufkens, D. J. *Coord. Chem. Rev.* **1990**, *104*, 39.
(22) Balk, R. W.; Snoeck, T. L.; Stufkens, D. J.; Oskam, A. *Inorg. Chem.* **1980**, *19*, 3015.
(23) van Koten, G.; Vrieze, K. *Adv. Organomet. Chem.* **1982**, *21*, 151.
(24) Kaim, W.; Klein, A.; Hasenzahl, S.; Stoll, H.; Zalis, S.; Fiedler, J. *Organometallics* **1998**, *17*, 237.
(25) Hasenzahl, S.; Hausen, H.-D.; Kaim, W. *Chem.—Eur. J.* **1995**, *1*, 95.
(26) Klein, A.; Hausen, H.-D.; Kaim, W. *J. Organomet. Chem.* **1992**, *440*, 207.
(27) Scott, J. D.; Puddephatt, R. J. *Organometallics* **1983**, *2*, 1643.
(28) Eaborn, C.; Kundu, K.; Pidcock, A. *J. Chem. Soc., Dalton Trans.* **1981**, 933.

(d, 12 H, ^3J = 6.59 Hz, CH(CH_3)$_2$), 2.34 (s, 4H, $^2J_{Pt-H}$ = 84 Hz, Pt−CH_2−), 4.95 (septet, 2H, CH(CH$_3$)$_2$), 9.22 (s, 2H, $^3J_{Pt-H}$ = 32.4 Hz, H$_{imino}$).

[(*i*Pr-DAB)Pt(neoSi)$_2$] (neoSi = Neosilyl or Trimethylsilylmethyl). From [(NBD)Pt(neoSi)$_2$], T = 333 K, time 120 h. Yield (violet powder): 74% (conversion 50%). Anal. Calcd for $C_{16}H_{38}N_2Si_2Pt$: C, 37.70; H, 7.51; N, 5.50%. Found: C, 37.69; H, 7.49; N, 5.47%. ^{1}H NMR (CD_2Cl_2) δ (ppm): −0.07 (s, 18 H, Si(CH_3)$_3$), 1.34 (s, 4H, $^2J_{Pt-H}$ = 87.6 Hz, Pt−CH_2−), 1.43 (d, 12 H, ^3J = 6.6 Hz, CH(CH_3)$_2$), 4.69 (septet, 2H, CH(CH_3)$_2$), 9.13 (s, 2H, $^3J_{Pt-H}$ = 39.7 Hz, H$_{imino}$).

[(*i*Pr-DAB)Pt(adme)$_2$] (adme = 1-Adamantylmethyl). From [(COD)Pt(adme)$_2$], T = 363 K, time 18 h. Yield (blue powder): 88%. Anal. Calcd for $C_{30}H_{50}N_2Pt$: C, 56.85; H, 7.95; N, 4.42%. Found: C, 56.71; H, 7.91; N, 4.38%. ^{1}H NMR (C_6D_6) δ (ppm): 1.09 (d, 12 H, ^3J = 6.57 Hz, CH(CH_3)$_2$), 1.48 (d, 12 H, J = 2.68 Hz, Ad$^{\epsilon CH_2}$), 1.68 (m, 12H, Ad$^{\gamma CH_2}$), 1.82 (s, 4H, $^2J_{Pt-H}$ = 88.76 Hz, Pt−CH_2−), 2.11 (m, 6H, Ad$^{\delta CH}$), 4.99 (septet, 2H, CH(CH$_3$)$_2$), 8.32 (s, 2H, $^3J_{Pt-H}$ = 32 Hz, H$_{imino}$).

[(*i*Pr-DAB)Pt(Ph)$_2$]. From [(COD)Pt(Ph)$_2$] in toluene, T = 393 K, time 48 h. Yield (red powder): 91%. Anal. Calcd for $C_{20}H_{26}N_2Pt$: C, 49.07; H, 5.35; N, 5.72%. Found: C, 49.01; H, 5.32; N, 5.70%. ^{1}H NMR ($CDCl_3$) δ (ppm): 1.19 (d, 12 H, ^3J = 6.6 Hz, CH(CH_3)$_2$), 4.24 (septet, 2H, CH(CH$_3$)$_2$), 6.75 (t, 2H, $^3J_{pPh-mPh}$ = 7.2 Hz, *p*-Ph), 6.92 (dd, 4H, $^3J_{mPh-oPh}$ = 6.9 Hz, *m*-Ph), 7.34 (d, 4H, $^3J_{Pt-H}$ = 69.5 Hz, *o*-Ph), 8.82 (s, 2H, $^3J_{Pt-H}$ = 34.5 Hz, H$_{imino}$).

[(*i*Pr-DAB)Pt(Mes)$_2$]. From [(dmso)$_2$Pt(Mes)$_2$] in toluene, T = 393 K, time 72 h. Yield (violet powder): 85%. Anal. Calcd for $C_{26}H_{38}N_2Pt$: C, 54.43; H, 6.68; N, 4.88%. Found: C, 54.35; H, 6.63; N, 4.86%. ^{1}H NMR ($CDCl_3$) δ (ppm): 1.20 (d, 12 H, ^3J = 6.57 Hz, CH(CH_3)$_2$), 2.17 (s, 6H, *p*-CH_3), 2.31 (s, 12H, $^4J_{Pt-H}$ = 5.7 Hz, *o*-CH_3) 3.99 (septet, 2H, CH(CH$_3$)$_2$), 6.55 (s, 4H, $^4J_{Pt-H}$ = 15 Hz, H-Mes), 8.94 (s, 2H, $^3J_{Pt-H}$ = 36.3 Hz, H$_{imino}$).

[(*i*Pr-DAB)Pt(C≡C^{t}Bu)$_2$]. From [(COD)Pt(C≡C^{t}Bu)$_2$] in toluene, T = 373 K, time 72 h. Yield (violet powder): 90%. Anal. Calcd for $C_{20}H_{34}N_2Pt$: C, 48.28; H, 6.89; N, 5.63%. Found: C, 48.29; H, 6.90; N, 5.66%. ^{1}H NMR ($CDCl_3$) δ (ppm): 1.24 (s, 18H, C(CH_3)$_3$), 1.55 (d, 12H, ^3J = 6.65 Hz, CH(CH_3)$_2$), 4.76 (septet, 2H, CH(CH$_3$)$_2$), 8.63 (s, 2H, $^3J_{Pt-H}$ = 48.2 Hz, H$_{imino}$).

[(*i*Pr-DAB)Pt(C≡CPh)$_2$]. From [(COD)Pt(C≡CPh)$_2$] in toluene, T = 373 K, time 60 h. Yield (brown powder): 92%. Anal. Calcd for $C_{24}H_{26}N_2Pt$: C, 53.62; H, 4.88; N, 5.21%. Found: C, 53.87; H, 4.90; N, 5.31%. ^{1}H NMR ($CDCl_3$) δ (ppm): 1.56 (d, 12 H, ^3J = 6.43 Hz, CH(CH_3)$_2$), 4.86 (septet, 2H, CH(CH$_3$)$_2$), 7.08 (dt, 2H, $^3J_{pPh-mPh}$ = 7.35 H, $^4J_{pPh-oPh}$ = 1.37 Hz, *p*-Ph), 7.20 (dd, 4H, $^3J_{mPh-oPh}$ = 7.58 Hz, *m*-Ph), 7.38 (d, 4H, *o*-Ph), 8.70 (s, 2H, $^3J_{Pt-H}$ = 50.7 Hz, H$_{imino}$).

Physical Measurements. ^{1}H NMR spectra were recorded on Bruker AC 250 or Varian Mercury 300 spectrometers. UV−vis absorption spectra were recorded on Bruins Instruments Omega 10, Hewlett-Packard 8453 Diode Array, and Varian Cary 4E spectrophotometers. Resonance Raman spectra of the complexes dispersed in KNO_3 pellets were recorded on a Dilor XY spectrometer equipped with a Wright Instruments CCD detector, using Spectra Physics 2040E Ar^+ and Coherent CR490 and CR590 dye lasers (with stilbene, Coumarin 6, and Rhodamine 6G dyes) as excitation sources. The photoreactions were performed by irradiation of solutions in CD_2Cl_2 (Cambridge Isotope Laboratories, 99.9%D) with an Oriel 6137 high pressure Hg lamp with a suitable cutoff filter for product analysis by ^{1}H NMR, or in degassed CH_2Cl_2 solutions using a Spectra Physics 2040E Ar^+ laser for the determination of quantum yields. Calibration was affected using Aberchrome 540.

Computational Details. The ground-state electronic structure calculations on complexes [(*i*Pr-DAB)Pt(R)$_2$] (R = CH_3, *i*Pr, C≡CH, or Ph) were performed using density functional theory (DFT) methods using the ADF2000.2[29,30] and Gaussian 98[31] program packages. The lowest-energy electronic transitions of (model) complexes [(*i*Pr-DAB)Pt(CH$_3$)$_2$], [(*i*Pr-DAB)Pt(Ph)$_2$], and [(*i*Pr-DAB)Pt(C≡CH)$_2$] were calculated by the time-dependent DFT (TD DFT) method (both ADF and Gaussian 98). The electrostatic solvent effect was simulated by the polarizable continuum model[32] incorporated into Gaussian 98. This model defines the solvent cavity as a union of interlocking atomic spheres.

Gaussian 98 was used for the calculations of the vibrations of [(*i*Pr-DAB)Pt(CH$_3$)$_2$], [(*i*Pr-DAB)Pt(CD$_3$)$_2$], [(*i*Pr-DAB)Pt(Ph)$_2$], and [(*i*Pr-DAB)Pt(C≡CMe)$_2$].

Within the ADF program, Slater-type orbital (STO) basis sets of triple ζ quality with polarization functions were employed. The inner shells were represented by the frozen core approximation (1s for C and N and 1s−4d for Pt were kept frozen). The following density functionals were used within ADF: the local density approximation (LDA) with VWN parametrization of electron gas data or the functional including Becke's gradient correction[33] to the local exchange expression in conjunction with Perdew's gradient correction[34] to the LDA expression (ADF/BP). The scalar relativistic zero order regular approximation (ZORA)[35] was used in this study.

Within Gaussian 98, Dunning's polarized valence double ζ basis sets[36] were used for C, N, and H atoms, and the quasirelativistic effective core pseudopotentials and corresponding optimized set of basis functions[37] were used for Pt. Becke's hybrid three parameter functional with the Lee, Yang, and Parr correlation functional (B3LYP)[38] was used in Gaussian 98 calculations.

The calculations on [(*i*Pr-DAB)Pt(R)$_2$] were performed in C_{2v} constrained symmetry (C_2 for R = Ph), with the z axis coincident with C_2 symmetry axis and the central atoms of the R substituents in the yz plane. All results discussed correspond to optimized geometries. For R = Ph, the tilt angle was calculated to 65.1°. This angle is found in diarylplatinum complexes of diimines to vary from 65° to 70° in good agreement with the calculated value.[8,26,39,40]

(29) Fonseca Guerra, C.; Snijders, J. G.; Te Velde, G.; Baerends, E. J. *Theor. Chim. Acta* **1998**, *99*, 391.
(30) Van Gisbergen, S. J. A.; Snijders, J. G.; Baerends, J. L. *Comput. Phys. Commun.* **1999**, *118*, 119.
(31) Frisch, M. J.; Trucks, G. W.; Schlegel, H. B.; Scuseria, G. E.; Robb, M. A.; Cheeseman, J. R.; Zakrzewski, V. G.; Montgomery, J. A., Jr.; Stratmann, R. E.; Burant, J. C.; Dapprich, S.; Millam, J. M.; Daniels, A. D.; Kudin, K. N.; Strain, M. C.; Farkas, O.; Tomasi, J.; Barone, V.; Cossi, M.; Cammi, R.; Mennucci, B.; Pomelli, C.; Adamo, C.; Clifford, S.; Ochterski, J.; Petersson, G. A.; Ayala, P. Y.; Cui, Q.; Morokuma, K.; Malick, D. K.; Rabuck, A. D.; Raghavachari, K.; Foresman, J. B.; Cioslowski, J.; Ortiz, J. V.; Stefanov, B. B.; Liu, G.; Liashenko, A.; Piskorz, P.; Komaromi, I.; Gomperts, R.; Martin, R. L.; Fox, D. J.; Keith, T.; Al-Laham, M. A.; Peng, C. Y.; Nanayakkara, A.; Gonzalez, C.; Challacombe, M.; Gill, P. M. W.; Johnson, B.; Chen, W.; Wong, M. W.; Andres, J. L.; Gonzalez, C.; Head-Gordon, M.; Replogle, E. S.; Pople, J. A. *Gaussian 98*, revision A.6; Gaussian Inc.: Pittsburgh, PA, 1998.
(32) Amovilli, C.; Barone, V.; Cammi, R.; Cances, E.; Cossi, M.; Mennucci, B.; Pomelli, C. S.; Tomasi, J. *Adv. Quantum Chem.* **1999**, *32*, 227.
(33) Becke, A. D. *Phys. Rev. A* **1988**, *38*, 3098.
(34) Perdew, J. P. *Phys. Rev. A* **1986**, *33*, 8822.
(35) van Lenthe, E.; Ehlers, A.; Baerends, E.-J. *J. Chem. Phys.* **1999**, *110*, 8943.
(36) Woon, D. E.; Dunning, T. H. J. *J. Chem. Phys.* **1993**, *98*, 1358.
(37) Andrae, D.; Haeussermann, U.; Dolg, M.; Stoll, H.; Preuss, H. *Theor. Chim. Acta* **1990**, *77*, 123.
(38) Stephens, P. J.; Devlin, F. J.; Cabalowski, C. F.; Frisch, M. J. *J. Phys. Chem.* **1994**, *98*, 11623.

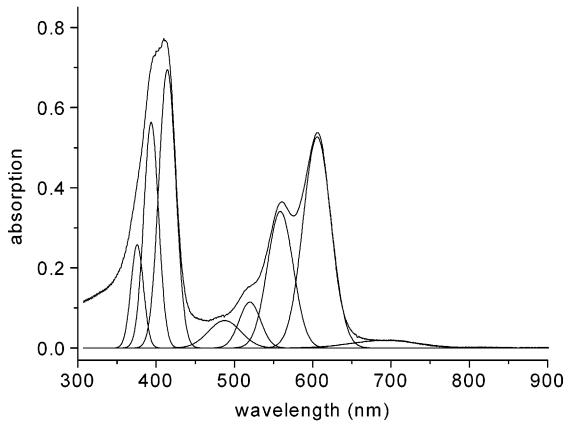

Figure 1. Absorption spectrum of [(^{i}Pr-DAB)Pt(CH_3)$_2$] in pentane and spectral deconvolution.

Results and Discussion

After briefly discussing the syntheses of the complexes, this section continues with the results of calculations of the electronic structure and transitions. Experimental evidence for the assignment of the absorption spectra comes from the rR spectra in combination with DFT calculations. The section concludes with the photochemical properties of the complexes.

Synthesis and Characterization. All complexes were prepared from precursors of the type [(L)$_2$Pt(R)$_2$], where L = dmso, $^1/_2$ COD (COD = 1,5-cyclooctadiene), or $^1/_2$ NBD (NBD = norbornadiene). The R = Mes complex can only be prepared from the precursor complex with L = dmso, which has been reported for the dimesityl-platinum(II) complexes of other α-diimine ligands.[11,24] The complexes with R = neop, neoSi, and CD_3 are best prepared from the NBD precursor, where use of the COD complex leads to extensive decomposition. The other complexes can be prepared from both the COD and the NBD precursors. It was found that often the best results were obtained if the reactions were only driven to 50% conversion of the diolefin platinum precursor. Starting compound and product can then be separated by careful recrystallization. Introduction of very σ donating substituents such as benzyl or isopropyl failed using the same procedure as that previously described and also failed using direct alkylation attempts with [(^{i}Pr-DAB)-Pt(Cl)$_2$] and RMgBr. Similar findings have been reported in the literature.[2] A reasonable explanation is that the strong trans effect of such strong σ donor R ligands might give rise to diimine abstraction and decomposition of the complex.

Optical Spectroscopy. Figure 1 shows the absorption spectrum of [(^{i}Pr-DAB)Pt(CH_3)$_2$] in *n*-pentane, as a representative example of the whole series of complexes. The absorption bands of all complexes can be divided into two distinct sets, one in the visible and one in the (near) UV. Hereafter, these are called band systems I and II, respectively. In Table 1, the absorption maxima of all compounds in nonpolar solvents are given. The maxima of the absorption bands in band system I are called $\lambda_1-\lambda_3$, while the main maximum of band system II is given under λ_4. Furthermore, the maxima λ_1 and λ_2 as measured in very polar solvents are given to demonstrate the negative solvatochromism, indicating that the corresponding electronic transitions have charge transfer character. The extent of solvatochromism for the first two bands ($\Delta\nu$) varies with the character of the R group and is also not identical for λ_1 and λ_2. In previous work, we have assigned the observed structuring of band system I in complexes [(R′-DAB)Pt(CH_3)$_2$] (R′ = ^{t}Bu, Tol, Xyl) to vibrational coupling.[24,25] However, the systems reported therein showed pronounced structure only in very nonpolar solvents. The present systems [(^{i}Pr-DAB)Pt(R)$_2$] with R = alkyl also allow the observation of structure in polar solvents that is probably due to their structural simplicity. Thus, these new results indicate a different electronic transition to be the origin for the two maxima rather than vibrational coupling. The alkyl substituted complexes possess only one strong band in the UV, while those with unsaturated co-ligands show additional bands, which are attributable to $\pi-\pi^*$ transitions. The absorption spectra of these latter complexes are generally more complex than those of the former, leading to partial overlap of the two band systems. To assign the observed absorption bands, DFT calculations on the electronic structure and transitions were performed which are reported in following paragraphs.

Electronic Structure and Transitions. The influence of the σ donating abilities of an alkyl substituent on the electronic structure was investigated by calculating orbital energies and compositions of [(^{i}Pr-DAB)Pt(R)$_2$] with R = Me, ^{i}Pr. As two examples of complexes with unsaturated co-ligands, the same calculations were performed on the compounds with R = C≡CH and Ph.

In Table 2, the results of the ADF/BP calculations for the methyl and isopropyl complexes are reported. The compositions of the frontier orbitals calculated by G98/B3LYP are similar. It is clear from this table that for both alkyl complexes the highest occupied four MOs have predominant platinum character, with significant contributions of the sp^3(R) orbitals, whereas the two lowest unoccupied MOs are mainly formed by the π^*(^{i}Pr-DAB) orbital. They have a significant platinum contribution as in the corresponding COD complexes, where the LUMO is the π^*(COD) level.

Figures 2 and 3 depict the HOMO and LUMO of [(^{i}Pr-DAB)Pt(CH_3)$_2$], respectively. From Figure 2, it is clear that the d(Pt)−sp^3(CH_3) interaction in the HOMO is bonding. The clearest difference between the Me and ^{i}Pr complexes is found in the alkyl group contribution to the HOMO which changes from 12% to 24% going from the former to the latter. Concurrently, this orbital rises in energy by about 4 × 10^3 cm^{-1} (1 eV ≈ 8 × 10^3 cm^{-1}). The absolute contribution of the alkyl group to the HOMO has decreased roughly twofold for these ^{i}Pr-DAB complexes compared to the corresponding COD ones (31% and 43% for R = Me and ^{i}Pr, respectively).[19]

The TD DFT (Gaussian 98) calculated transition energies (Table 3) show that indeed the lowest-energy transitions in [(^{i}Pr-DAB)Pt(CH_3)$_2$] occur from the HOMOs to the π^*(^{i}Pr-

(39) Klein, A.; McInnes, E. J. L.; Kaim, W. *J. Chem. Soc., Dalton Trans* **2002**, 2371.
(40) Klein, A.; Kaim, W.; Waldhoer, E.; Hausen, H.-D. *J. Chem. Soc., Perkin Trans. 2* **1995**, 2121.

Table 1. Observed Electronic Absorption Maxima for Complexes [(^{i}Pr-DAB)Pt(R)$_2$][a]

	solvent = pentane or hexane				solvent = DMF			
R	$\lambda_4(\epsilon)$	$\lambda_3(\epsilon)$	$\lambda_2(\epsilon)$	$\lambda_1(\epsilon)$	λ_2	λ_1	$\Delta\nu_2$ [cm^{-1}]	$\Delta\nu_1$ [cm^{-1}]
adme	418 (2.77)	531 (1.14)	576 (1.84)	619 (2.24)	540	569	1160	1420
neop	418 (3.06)	530 (1.19)	575 (2.02)	617 (2.57)	529[b]	567[b]	1512	1430
neoSi	412 (2.81)	519 (0.92)	561 (1.61)	609 (2.10)	501	529	2130	2480
CH_3	390 (3.34)	518 (1.02)	560 (2.00)	606 (2.47)	513	538	1640	2090
Mes	367 (3.38)	484 (3.36)	517 (3.46)	558 (3.63)	491	512	1030	1610
Ph	386 (4.27)[c]	504 (1.81)	549 (2.19)	596 (2.50)	457[b]	495[b]	3370	3420
C≡C^{t}Bu	409 (3.24)[d]	440 (3.31)	490 (2.64)	528 (3.20)	426	468	3070	2430
C≡CPh	321 (16.2)	398 (8.95)	452 (5.30)	515 (3.73)	410	443	2270	3160

[a] Absorption maxima wavelengths are given in nm; the molar extinction coefficients ϵ are given in parentheses (in 1000 M^{-1}cm^{-1}). Solvatochromic shift $\Delta\nu$ ($\equiv\nu$(DMF) − ν(alkane)) values are given in cm^{-1}. [b] Measured in MeCN. [c] Further close lying maxima: 448 nm (ϵ = 1980 M^{-1} cm^{-1}), 372 nm (ϵ = 4260 M^{-1} cm^{-1}). [d] Further maxima: 388 nm (3022 M^{-1} cm^{-1}) and 369sh nm.

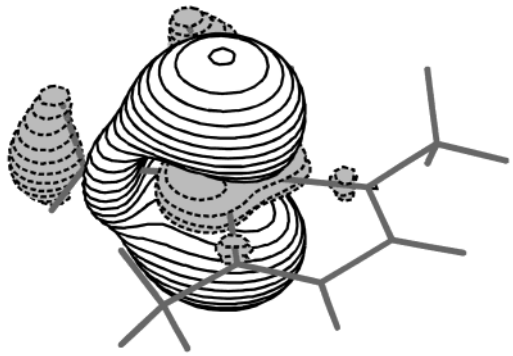

Figure 2. 19a$_1$ HOMO of [(^{i}Pr-DAB)Pt(CH$_3$)$_2$].

Table 2. ADF/BP Calculated One-Electron Energies and Percentage Composition of Selected Highest Occupied and Lowest Unoccupied Molecular Orbitals of [(^{i}Pr-DAB)Pt(R)$_2$] (R = CH$_3$ or ^{i}Pr (in Parentheses)) Expressed in Terms of Composing Fragments

MO	E (eV)	prevailing character	Pt	R	^{i}Pr-DAB
		Unoccupied			
16b$_2$	0.21	d_{Pt} + R	2 p_y; 35 d_{yz}	48	15
9a$_2$	−0.30	π^* DAB	1 d_{xy}		98
11b$_1$ (14b$_1$)	−3.37 (−3.34)	π^* DAB + d_{Pt}	18 (16) d_{xz}; 1 (1) p_x	2 (2)	78 (81) π^*
		Occupied			
19a$_1$ (22a$_1$)	−4.77 (−4.27)	d_{Pt} + R	21 (24) s; 63 (44) $d_{x^2-y^2}$; 3 (8) d_{z^2}	12 (24)	
8a$_2$ (11a$_2$)	−4.79 (−4.60)	d_{Pt}	82 (85) d_{xy}	7 (6)	10 (7)
18a$_1$ (21a$_1$)	−5.21 (−5.16)	d_{Pt} + R	4 (2) s; 72 (67) d_{z^2}; 5 (10) $d_{x^2-y^2}$	12 (13)	4 (6)
10b$_1$ (10b$_1$)	−5.43 (−5.43)	d_{Pt} + DAB	68 (74) d_{xz}; 1 (0) p_x	7 (5)	24 (21)
7a$_2$ (7a$_2$)	−7.12 (−7.07)	DAB	6 (3) d_{xy}	4 (10)	89 (87)

DAB) LUMO. Hence, they are mainly MLCT in character. Because of the admixture of the sp^3(CH$_3$) orbitals to the HOMOs, the lowest-energy transitions remove electron density from the σ(Pt−C) bond. Transitions that remove electron density from bonding metal−ligand orbitals have been named σ-bond-to-ligand charge transfer (SBLCT) transitions.[19,41,42] As the methyl group contribution to the HOMO diminishes going from the COD to the ^{i}Pr-DAB complexes, a relatively lower photoreactivity for the ^{i}Pr-DAB complexes is expected (see later).

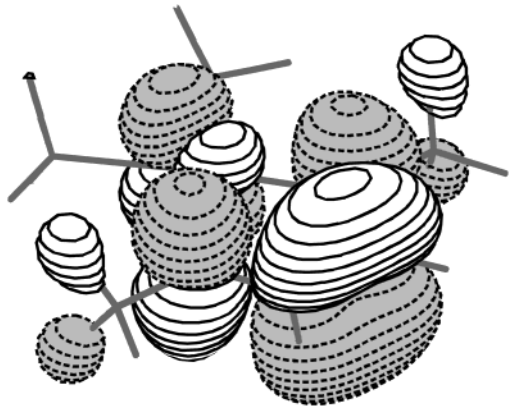

Figure 3. 11b$_1$ LUMO of [(^{i}Pr-DAB)Pt(CH$_3$)$_2$].

Table 3. Selected G98/B3LYP Calculated Lowest TD DFT Singlet Excitation Energies (eV) for [(^{i}Pr-DAB)Pt(CH$_3$)$_2$] and Experimental Absorption Maxima

		G98/B3LYP (CH_2Cl_2)[a]		exptl
state	main character	trans. energy eV (nm)	osc str	λ_{max} nm[b] (ϵ M^{-1}cm^{-1})
^{1}B$_1$	98% 19a$_1$ → 11b$_1$	1.99 (625)	0.0016	543 (2470)
^{1}B$_2$	99% 8a$_2$ → 11b$_1$	2.09 (595)	0.0	507 (2000)
^{1}B$_1$	98% 18a$_1$ → 11b$_1$	2.46 (505)	0.0001	470 (1020)
^{1}A$_1$	94% 10b$_1$ → 11b$_1$	3.12 (398)	0.113	390 (3340)
^{1}B$_2$	86% 7a$_2$ → 11b$_1$	4.99 (249)	0.157	245 (7800)

At higher energies, first a pure MLCT and then an ^{i}Pr-DAB intraligand (IL) transition are found. The lowest-energy absorption bands (band system I in the absorption spectra) are very solvatochromic. To decrease the difference between calculated and observed transition energies, the effect of the solvent was simulated by the polarizable continuum model included in the Gaussian 98 program (see Experimental Section). This led to an increase in calculated transition energies. The fact that for the three lowest transitions they are still appreciably lower than the observed ones implies that this simple model does not simulate the solvent effect well. In DFT calculations on several other complexes, calculated transition energies that are too low were found as well.[43,44] The calculated and observed transition energies for the other two, less solvatochromic, transitions (Table 3) correspond much better. The calculated oscillator strengths of the three

(41) Niewenhuis, H. A.; Stufkens, D. J.; McNicholl, R. A.; Al-Obaidi, A. H. R.; Coates, C. G.; Bell, S. E. J.; McGarvey, J. J.; Westwell, J.; George, M. W.; Turner, J. J. *J. Am. Chem. Soc.* **1995**, *117*, 5579.
(42) Djurovich, P. I.; Watts, R. J. *Inorg. Chem.* **1993**, *32*, 4681.
(43) Turki, M.; Daniel, C.; Záliš, S.; Vlcek, A. J.; van Slageren, J.; Stufkens, D. J. *J. Am. Chem. Soc.* **2001**, *123*, 11431.
(44) Van Slageren, J.; Stufkens, D. J.; Záliš, S.; Klein, A. *J. Chem. Soc., Dalton Trans.* **2002**, 218.

Table 4. ADF/BP Calculated One-Electron Energies and Percentage Composition of Selected Highest Occupied and Lowest Unoccupied Molecular Orbitals of [(^{i}Pr-DAB)Pt(C≡CH)$_2$] Expressed in Terms of Composing Fragments

MO	E (eV)	prevailing character	Pt	C≡CH	^{i}Pr-DAB
		Unoccupied			
$17b_2$	−0.68	d_{Pt} + CCH + ^{i}Pr-DAB	8 p_y; 38 d_{yz}	30	23
$9a_2$	−0.65	π^* ^{i}Pr-DAB	1 d_{xy}		98
$11b_1$	−3.91	π^* ^{i}Pr-DAB + d_{Pt}	12 d_{xz}	10	78 π^*
		Occupied			
$8a_2$	−5.08	CCH + d_{Pt}	32 d_{xy}	65	3
$20a_1$	−5.18	CCH + d_{Pt}	15 d_{z^2}; 10 $d_{x^2-y^2}$	74	2
$10b_1$	−5.58	CCH + d_{Pt} + ^{i}Pr-DAB	20 d_{xz}; 2 p_x	62	16
$16b_2$	−5.62	CCH		98	2
$19a_1$	−5.79	d_{Pt}	21 s; 52 $d_{x^2-y^2}$; 23 d_{z^2}	3	2
$7a_2$	−7.35	d_{Pt} + CCH + ^{i}Pr-DAB	35 d_{xy}	34	31

lowest-energy transitions are much lower than expected on the basis of the observed extinction coefficients. However, in view of the transition energies, we feel confident that our present assignment of the observed absorption bands to these calculated transitions is the correct one. Hence, this discrepancy must be due to factors that were not taken into account in the TD DFT calculations, such as spin−orbit coupling due to the platinum atom, the influence of vibrational motion of the molecule which can increase orbital overlap, electronic through-solvent interaction, and so on. In conclusion, the calculations suggest that the observed structure of the absorption bands in band system I is due to the presence of different electronic transitions rather than vibrational fine structure. This conclusion is different from that given in a previous paper, as calculation methods have improved greatly over the past few years, which makes unambiguous assignment of electronic transitions to absorption bands now possible.

The electronic structure of the complexes with unsaturated co-ligands is different from that of the alkyl ones. Whereas the co-ligand contribution to the highest filled MOs is relatively small in the latter complexes, it is the major contribution in the former ones. The ADF/BP calculated orbital characters and energies of the [(^{i}Pr-DAB)Pt(C≡CH)$_2$] model complex (Table 4) show that the four highest occupied orbitals all have over 60% alkynyl character, with the platinum center contributing about 20−30% to the three highest ones and not at all to the fourth. Recent IEH calculations (IEH = iterative extended Hückel) on [(phen)-Pt(C≡CR)$_2$] (phen = 1,10-phenanthrolines, R = H, F, or Ph) show lower contributions (around 20%) of the alkynyl groups to high lying filled orbitals.[4] The different calculation approach is proposed to be the reason for this difference, particularly the fact that the semiempirical extended Hückel method does not take into account the electron correlation. The LUMO is mainly formed by the π^*(^{i}Pr-DAB) orbital. These results are very similar to those obtained for the corresponding COD complex.[19]

In view of the orbital composition of the HOMOs (Figure 4), the low-lying electronic transitions have mixed MLCT/L′LCT character, where L′LCT denotes charge transfer from the alkynyl ligand to the ^{i}Pr-DAB one. Although the orbital $8a_2$ (Table 4) is the HOMO, the lowest-energy transition is calculated to be the HOMO−1 → LUMO one (Table 5). This makes the order of the electronic transitions the same as that of the alkyl complexes. In addition, one extra transition is calculated, which has partial IL(C≡CH) character but is rather mixed. The calculated energies of the three lowest-energy transitions are lower than those of the observed absorption bands, because of reasons similar to those described previously and, in this case, possibly also because the calculations were performed on a model complex. In the alkynyl complex too, the oscillator strengths are lower than expected when looking at the extinction coefficients. Again, our assignment seems to be the only reasonable one on the basis of these calculations. In contrast, in the literature, the HOMO of alkynyl−platinum(II)−diimine complexes has been thought to be primarily metal based on the basis of the observation that the emission energy decreases with increasing donor strength of the alkynyl ligand.[3,4,9] DFT and TD DFT calculations on [(^{i}Pr-DAB)Pt(Ph)$_2$] showed that also the phenyl group participates in the lowest-energy electronic transitions of the complex, albeit to a lower extent than the alkynyl ones (for details see Supporting Information).

Summarizing, in all the present complexes, the co-ligand orbitals play a significant role in the HOMOs and therefore in the low-lying electronic transitions, in contrast to what is generally assumed for such complexes. A technique to obtain experimental evidence about the nature of the electronic transitions responsible for the observed absorption band is resonance Raman (rR) spectroscopy. The results of an rR study on these complexes are reported in the following paragraphs.

Resonance Raman. The rR spectra of the [(R′-DAB)-Pt(R)$_2$] (R = CH_3, R′ = ^{i}Pr, cHx, *p*-Tol; R = CD_3, C≡C^{t}Bu, Mes, R′ = ^{i}Pr) complexes dispersed in KNO_3 were recorded on irradiation into their lowest-energy absorption bands. The rR technique is based on the fact that only those Raman bands which are due to vibrations influenced by the electronic transition that is excited are resonantly enhanced in intensity.[45] There are several instances in which resonance Raman was used to distinguish several electronic transitions within an apparently single absorption band.[46−48]

Figure 5 depicts typical resonance Raman spectra for these complexes. In each case, there is one very strong resonance around that ranges from 1514 cm^{-1} for R = adme to 1559 cm^{-1} for R = C≡C^{t}Bu. This band is assigned to the ν_s(CN) vibration of the DAB ligand in agreement with other studies on such complexes.[41,44,49] The energy of the band increases parallel to the series adme < neop < CD_3 < CH_3 < Mes <

(45) Clark, R. J. H.; Dines, T. J. *Angew. Chem., Int. Ed. Engl.* **1986**, *25*, 131.
(46) Egolf, D. S.; Waterland, M. R.; Kelley, A. M. *J. Phys. Chem. B* **2000**, *104*, 10727.
(47) Balk, R. W.; Stufkens, D. J.; Oskam, A. *Inorg. Chim. Acta* **1979**, *34*, 267.
(48) Shin, K.-S. K.; Zink, J. I. *J. Am. Chem. Soc.* **1990**, *112*, 7148.
(49) van Slageren, J.; Klein, A.; Záliš, S.; Stufkens, D. J. *Coord. Chem. Rev.* **2001**, *219−221*, 937.

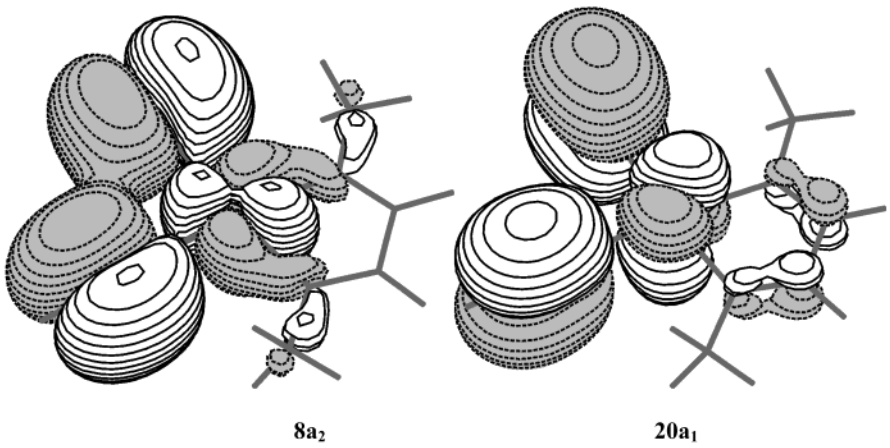

Figure 4. $8a_2$ HOMO and $20a_1$ HOMO − 1 of [(Me-DAB)Pt(C≡CH)$_2$].

Table 5. Selected Calculated Lowest TD DFT Singlet Excitation Energies (eV and nm) for [(^{i}Pr-DAB)Pt(C≡CH)$_2$] Together with Experimentally Observed Values for [(^{i}Pr-DAB)Pt(C≡C^{t}Bu)$_2$]

		G98/B3LYP		G98/B3LYP (CH_2Cl_2)		
state	main character	trans energy eV	osc. str.	trans energy, eV (nm)	osc str	exptl λ_{max} nm[a] (ϵ M^{-1} cm^{-1})
$^1B_1$	98% $20a_1 \rightarrow 11b_1$	1.58	0.0020	1.95 (638)	0.0032	477 (3250)
$^1B_2$	99% $8a_2 \rightarrow 11b_1$	1.91	0.0001	2.19 (566)	0.0002	438 (880)
$^1B_1$	98% $19a_1 \rightarrow 11b_1$	2.63	0.0002	2.89 (428)	0.0003	410 (750)
$^1A_1$	94% $10b_1 \rightarrow 11b_1$	3.18	0.095	3.29 (376)	0.092	393 (3240)
$^1B_2$	86% $20a_1 \rightarrow 17b_2$	4.65	0.079	4.94 (253)	0.036	295 (4310)
$^1A_1$	94% $8a_2 \rightarrow 9a_2$	5.02	0.187	4.92 (252)	0.144	268 (6580)

[a] From absorption spectra in CH_2Cl_2. Maxima and extinction coefficients were extracted from spectral deconvolution.

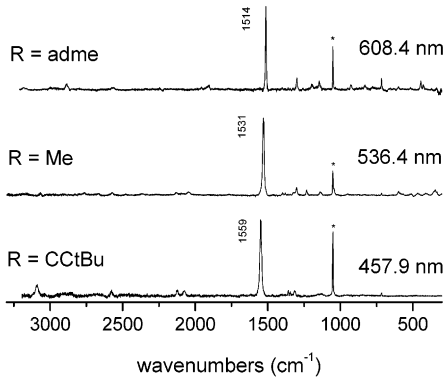

Figure 5. Resonance Raman spectra for [(^{i}Pr-DAB)Pt(R)$_2$] (R = adme, Me, or C≡C^{t}Bu) in KNO_3 pellets obtained on irradiation at the given irradiation wavelengths.

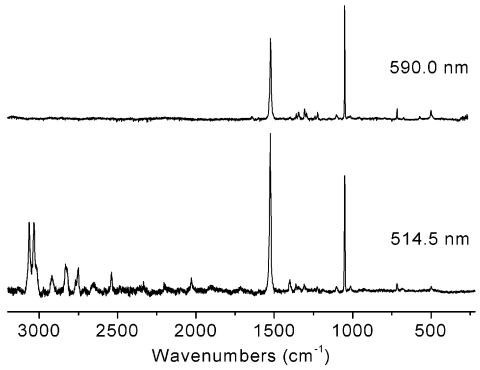

Figure 6. Resonance Raman spectra for [(cHx-DAB)Pt(CH_3)$_2$] in a KNO_3 pellet obtained upon irradiation at two different irradiation wavelengths.

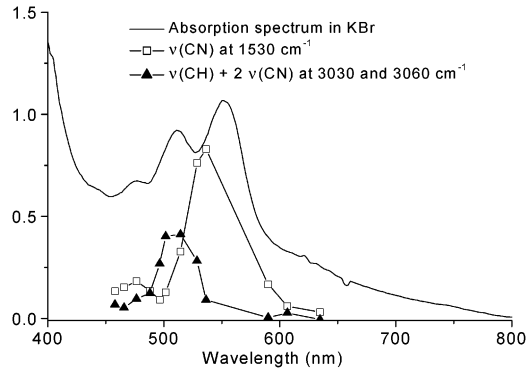

Figure 7. Resonance Raman excitation profile for [(cHx-DAB)Pt(CH_3)$_2$] in a KNO_3 pellet.

C≡C^{t}Bu. Decreasing electron donating power as represented by this series leads to decreased back-bonding to π^*(DAB), which is antibonding with respect to the C═N bond, with subsequent strengthening of the C═N bond. This resonance is shifted to lower energies for the complexes with aryl substituted R′-DAB ligands as shown here for [(*p*-Tol-DAB)-Pt(CH_3)$_2$] where the band is found at 1500 cm^{-1} (for full rR data, see Supporting Information). In this case, the aryl substituent causes weakening of the C═N bond by withdrawal of electron density from the (C═N bonding) π level of the R′-DAB ligand.

To probe for any difference between the electronic transitions belonging to the bands in band system I, rR spectra were obtained on irradiation at different excitation wavelengths. Figure 6 shows the rR spectra for [(cHx-DAB)-Pt(CH_3)$_2$] for the excitation wavelengths corresponding to the first and second absorption maxima. Clearly, the spectra are different depending on the excitation wavelength. Figure 7 shows the intensity of two typical bands of [(cHx-DAB)-Pt(CH_3)$_2$] as a function of the excitation wavelength (a so-called excitation profile), superimposed on an absorption spectrum in KBr, a matrix similar to KNO_3. The fact that Raman bands are enhanced irradiating into different bands of band system I proves beyond doubt that the absorption maxima belong to different transitions rather than being due to vibrational fine structure.

To assist in the assignment of the rR bands, DFT vibrational calculations were performed on complexes

Table 6. Experimental and Calculated Raman Bands for [(^{i}Pr-DAB)Pt(CH_3)$_2$] and [(^{i}Pr-DAB)Pt(CD_3)$_2$]

	R = CH_3		R = CD_3			
	exptl	calcd[a]	exptl	calcd[a]	assignment	trans[b]
1	3066				12 × 2 (3062/3056)	2
2	3030	3062	3030	3063	ν(CH) (imine)	2
3	2906	3001	2050	2089	ν(CH)/ν(CD) (Me)	2
4	2827				12 + 16 (2833)	2
5	2760				12 + 17 (2763)	2
6	2666				12 + 18 (2670)	2
7	2573				12 + 19 (2575)	2
8	2480				12 + 21 (2477)	2
9	2365				12 + 21 (2364)	2
10	2131				12 + 22 (2130)	2
11	2045				12 + 27 (2041)	1
12	1531	1531	1528	1532	ν(CN) (DAB)	1 + 2
13	1400	1402	1400	1403	δ(CH) (imine+^{i}Pr CH)	1
14	1379	1382	1377	1382	δ(CH) (^{i}Pr) + δ(CH) (imine)	1
15	1322	1324	1320	1325	δ(CH) (^{i}Pr) out of plane	1
16	1302	1312	1300	1311	δ(CH) (imine+^{i}Pr CH)	1
17	1232	1248	952	968	δ(CH_3)/δ(CD_3)(Me) + δ(CH) (^{i}PrDAB)	1
18	1139	1138	1138	1138	ν(CC) + δ(CH) (imine)	1
19	1044	1034	1042	1035	ν(CC) + δ(CH) (imine)	1
20	946w	928	942	929	δ(^{i}Pr-DAB) cycle	1
21	874w	863	660	628	δ(CH)/δ(CD) (Me) bend	1
22	833w	805	828	805	δ(^{i}Pr-DAB) cycle	1
23	599	582			ν(PtC) + ν(PtN)	1
24	575w	581			ν(PtC) + ν(PtN)	1
25	564w	571	508	509	ν(PtC)	1
27	510	487			δ(^{i}Pr-DAB) out of plane	1

[a] Calculated values were scaled by 0.97 using experimental (1531 cm^{-1}) and calculated (1579 cm^{-1}) values for ν_s(CN) for [(^{i}Pr-DAB)Pt(CH_3)$_2$]. [b] Enhanced for first or second transition.

[(^{i}Pr-DAB)Pt(R)$_2$] (R = CH_3, CD_3). Table 6 shows the experimental and calculated vibrations in addition to the assignments for these complexes. The ultimate column states whether the particular rR band belongs to the first or second electronic transition.

Starting with the assignment of the first electronic transition, the major band is clearly the one at 1531 cm^{-1} (R = CH_3) or 1528 cm^{-1} (R = CD_3). The observation of this ν_s(CN) band is clear evidence that the electronic transitions are directed toward the α-diimine ligand in all cases. The calculated value (1579 cm^{-1}) lies about 3% higher than the observed one. Such differences are quite normal using DFT techniques with the employed B3LYP functional. Indeed, a scaling factor of 0.961 was recommended in the literature.[50] To make a comparison between experimental and calculated values, all calculated values have been rescaled by 0.97. On irradiation into the lowest-energy absorption band, ν_s(CN) is the only strongly enhanced absorption band. Several others bands are visible, though. The ones between 1300 and 1400 cm^{-1} belong to imine CH and ^{i}Pr CH deformation vibrations, because they are observed at the same values for both the protonated and deuterated complexes and hence do not involve the platinum bound methyl groups. The band observed at 1232 cm^{-1} (R = CH_3) or 952 cm^{-1} (R = CD_3) clearly does. It was observed for other transition metal methyl complexes, such as [(^{i}Pr-DAB)Re(CH_3)(CO)$_3$], [(^{i}Pr-DAB)Ru(Cl)(R)(CO)$_2$] (R = CH_3, CD_3), [(^{i}Pr-DAB)Ru(R)($SnPh_3$)(CO)$_2$] (R = CH_3, CD_3), and [(^{i}Pr-DAB)Pt(R)$_4$] (R = CH_3, CD_3).[53] On the basis of calculations and the large influence of deuteration, it was assigned to an umbrella-like movement of the methyl groups. If the concerned methyl group is involved in the electronic transition to a large extent, this vibration shows up as a strongly enhanced band, such as in the case of [(^{i}Pr-DAB)Pt(CH_3)$_4$]. In the present [(^{i}Pr-DAB)Pt(R)$_2$] (R = CH_3, CD_3) complexes, it is only weakly enhanced, showing some but not major involvement of the methyl substituents in the lowest-energy electronic transition. This is in excellent agreement with the calculated sp^3(CH_3) contribution to the HOMO (12%). Furthermore, a Pt−CH_3 bending vibration (observed 874 cm^{-1} for R = CH_3 and at 660 cm^{-1} for R = CD_3) and a Pt−C stretching vibration (observed at 564 cm^{-1} for R = CH_3 and at 508 cm^{-1} for R = CD_3) are clearly influenced by deuteration. The weak bands at ca. 945 and 830 cm^{-1} belong to in-plane symmetric deformations of the ^{i}Pr-DAB ligand. They are resonantly enhanced whenever the electronic system becomes delocalized.[49] The fact that they are observed as weak bands means that this is not the case for these complexes, again in agreement with the DFT MO calculations (see previous description). Finally, combined symmetric Pt−C and Pt−N stretching vibrations are observed between 550 and 600 cm^{-1}.

The rR spectra observed on irradiation into the second absorption band are more particular. Whereas ν_s(CN) is still observed, its intensity is much weaker, indicating a smaller distortion along the CN coordinate in the excited state.[48,49,51] Furthermore, a number of bands are observed between 2000 and 3000 cm^{-1}. In this region, no molecular vibrations are calculated and indeed not expected. Upon closer inspection, they proved to be assignable to combination bands of ν_s(CN) with the various ligand and metal−ligand stretching and deformation vibrations, with the exception of the band at 3030 cm^{-1} that is assigned to the ν(CH) mode of the DAB ligand, in agreement with the lack of any deuteration effect.

In the rR spectrum of [(^{i}Pr-DAB)Pt(C≡C^{t}Bu)$_2$] upon irradiation into the second lowest absorption maximum, there is a strong enhancement of a band at 2132 cm^{-1} (Figure 8). We attribute this band to the C≡C stretching vibration ν(CC). This band is not enhanced when the compound is irradiated with lower energy, coincident with the lowest absorption maxima, where the strongest band is clearly the 1559 cm^{-1} resonance attributed to the ν_s(CN) vibration. From the calculations, it was found that the lowest electronic transition originates from an orbital that has different symmetry (HOMO − 1, $20a_1$) than the second transition (HOMO, $8a_2$) (Figure 4). This might be a qualitative explanation for the different rR behavior. In the related complex *trans*-[(dppm)$_2$Pt(C≡CPh)$_2$] (dppm = bis-diphenylphosphinomethane), the ν(CC) mode is also strongly enhanced (2114 cm^{-1}).[52] The authors explain this with a high

(50) Wong, M. W. *Chem. Phys. Lett*. **1996**, *256*, 391.

(51) Zink, J. I.; Shin, K.-S. K. *Molecular Distortions in Excited Electronic States Determined from Electronic and Resonance Raman Spectroscopy*; Volman, D. H., Hammond, G. S., Neckers, D. C., Eds.; Wiley: New York, 1991.

(52) Kwok, W. M.; Phillips, D. L.; Yeung, P. K.-Y.; Yam, V. W.-W. *Chem. Phys. Lett.* **1996**, *262*, 699.

(53) Weinstein, J.; van Slageren, J.; Stufkens, D. J.; Záliš, S.; George, M. W. *J. Chem. Soc., Dalton Trans.* **2001**, 2587.

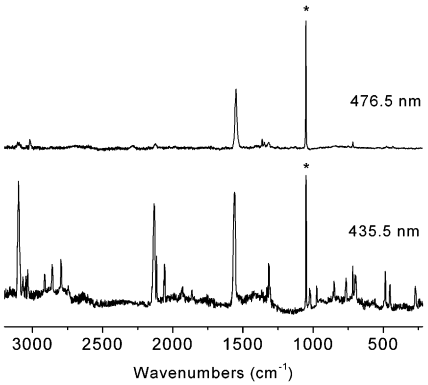

Figure 8. Resonance Raman spectra for [(^{i}Pr-DAB)Pt(C≡C^{t}Bu)$_2$] in a KNO_3 pellet obtained by irradiation at two different irradiation wavelengths. Asterisks denote NO_3^- bands.

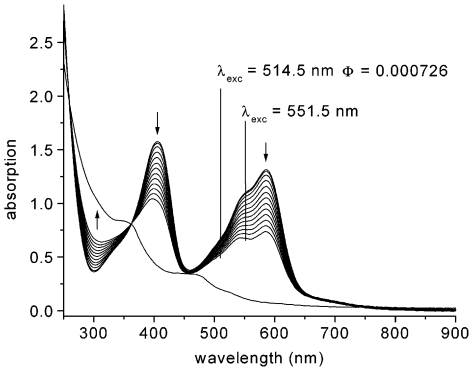

Figure 9. Absorption spectra of [(^{i}Pr-DAB)Pt(neop)$_2$] taken in CH_2Cl_2 during photolysis at $\lambda = 514.5$ nm. The traces are recorded after each 20 s of irradiation. The last spectrum represents [(^{i}Pr-DAB)Pt(Cl)(neop)].

contribution of the C≡C group to the radiationless decay from the MLCT excited state. However, for our system, such an explanation fails, because we found that the enhancement of the ν(CC) mode is excitation frequency dependent and does not occur upon irradiation into the lowest absorption band. Using time-resolved FTIR spectroscopy, Schanze et al. have found that the frequency of the ν(CC) modes in complexes [(R′-bpy)Pt(C≡CR)$_2$] (R = Aryl, R′-bpy = alkyl substituted bpy) are about 25−35 cm^{-1} higher in the excited states of the molecules than in their ground states which served as indication for an MLCT character of the excited state.[10] However, their investigations focus on the thermally relaxed excited state whereas rR provides direct information on the electronic transition. These can be quite different, as was recently shown by comparison of these two techniques.[53] From the striking agreement of our calculations and rR results, we conclude that the C≡CR group is directly involved in the electronic transition.

For the mesityl complex, the ν(CN) vibration is found at 1547 cm^{-1} in excellent agreement with the calculated value for [(^{i}Pr-DAB)Pt(Ph)$_2$] of 1541 cm^{-1} (see Table S3). With the help of this calculation, we were able to assign a number of resonantly enhanced bands that are located in the aryl substituent. These resonances, that were attributed to CH deformation modes (1462 and 1171 cm^{-1}), ν(CC) modes (1037, 1010, and 951 cm^{-1}) or to ring deformations (673 and 604 cm^{-1}), do not depend much on the irradiation wavelength, in agreement with the calculated electronic structure that reveals contributions of the aryl substituent to most of the highest occupied MOs.

Photochemistry. Both the (TD)DFT calculations and the rR spectra showed that while the low-lying electronic transitions of [(^{i}Pr-DAB)Pt(R)$_2$] (R = alkyl) complexes do possess some SBLCT character, the co-ligand contribution is much less than in the corresponding COD complexes.[19] This is expected to diminish the photoreactivity of the ^{i}Pr-DAB complexes. To investigate this expectation, their photoreactions were followed by ^{1}H NMR spectroscopy, irradiating 10^{-3} M solutions of the complexes in CD_2Cl_2 using a high pressure Hg lamp with a suitable cutoff filter to limit irradiation to band system I. The first observable products were the monochloro complexes [(^{i}Pr-DAB)Pt(Cl)(R)], characterized by the chemical shift and ^{195}Pt coupling constants. This suggests that the primary photochemical step is Pt−R bond homolysis followed by chlorine abstraction from the solvent. The photoreactions in non-chlorinated solvents are very unselective, giving rise to uninterpretable ^{1}H NMR spectra. In most cases, these latter photoreactions are accompanied by the formation of elemental platinum. To establish a relative series of efficiencies of the photoreactions depending on R, their photoreactions in CH_2Cl_2 solutions were followed by UV−vis spectroscopy, using the same irradiation method as in the NMR experiments. From the decay of the absorption band with irradiation time, the relative order of photoreaction efficiencies was determined to decrease along R = adme > neop > neoSi > CH_3, which is the same order as that found for the COD complexes.[19] The photoreactions of the [(^{i}Pr-DAB)Pt(neop)$_2$] complex were studied in more detail. First of all, it was found that upon irradiation at $\lambda > 600$ nm, to ensure that only the lowest-energy transition is excited, no photoreaction occurred, which means either that in the relaxed excited state the charge density decrease in the σ(Pt−R) is too low to weaken this bond enough to cause its rupture or that the excited state lifetime is too short. Indeed, the excited state lifetime was found to be <5 ns by transient absorption spectroscopy. In contrast, irradiation using 551.4 nm light from a Coumarine 6 dye laser (corresponding to the second absorption maximum) gave rise to measurable photoreactivity (Figure 9). This implies that in this case a prompt photochemical reaction occurs, that is, a photoreaction from a thermally nonrelaxed excited state which is fast enough to compete with vibrational relaxation.[54] The absolute photochemical quantum yield was determined by Ar^+ laser irradiation at 514.5 nm to be $\Phi = 7.3 \times 10^{-4}$. As in the case of the COD complexes, a relative increase in reactivity of a factor of 50 was found going from the Me to the neop compound; the photochemical quantum yield of [(^{i}Pr-DAB)Pt(CH$_3$)$_2$] is expected to be on the order of $\Phi = 10^{-5}$. The absolute photochemical quantum yield of [(COD)Pt(CH$_3$)$_2$] was determined to be $\Phi = 5 \times 10^{-3}$,[55] indicating that on going from the COD to the ^{i}Pr-DAB complexes the photoreactivity decreases 2 orders of magnitude.

(54) Langford, C. H. *Acc. Chem. Res.* **1984**, *17*, 96.
(55) Kunkely, H.; Vogler, A. *J. Organomet. Chem.* **1998**, *553*, 517.

The complexes with an unsaturated co-ligand (R = C≡C^{t}Bu, C≡CPh, Ph, Mes) are not photoreactive at all on irradiation into either band system I or band system II. This is not unexpected because the electronic transition does not remove electron density from the Pt—C bonds of these complexes, and they are therefore not weakened. The alkynyl derivatives show appreciable photoreactivity at much higher energy (λ > 320 nm) irradiation. According to NMR experiments as described previously, the photoproduct is the R′—C≡C−C≡C—R′ (R′ = ^{t}Bu or Ph) coupling product. In view of the elemental platinum formation that was observed in these experiments, this product is probably formed by reductive elimination as in the case of the corresponding COD complexes.

Conclusions

In this paper, a series of [(^{i}Pr-DAB)Pt(R)$_2$] (R = CH_3, CD_3, adme, neop, neoSi, C≡C^{t}Bu, C≡CPh, Ph, Mes) complexes was investigated. The aim was to determine to what extent the co-ligands are involved in low-lying electronic transitions with the ultimate goal to create complexes that are photoreactive on visible light irradiation. The co-ligand contribution proved to be significant in the case of alkyl co-ligands, while it is predominant when the co-ligands are unsaturated. This is an interesting conclusion because it is generally assumed that the co-ligands are not involved in the low-lying transitions and excited states of such complexes. Although the photoreactivity of the alkyl complexes can be significantly enhanced, on increasing the σ donor strength of the alkyl ligand, in an absolute sense it is too low for a reasonable application. The alkynyl complexes were found to be virtually photostable except when irradiated at relatively high energies.

Comparing results from (TD)DFT calculations on the electronic structure and low-lying transitions of the complexes to experimental information from electronic absorption and resonance Raman (rR) spectroscopies, it was found that the DFT methods predict the characters of low-lying electronic transitions well. However, the calculated energies and oscillator strengths are lower than those found experimentally. One other interesting result from both the calculations and the rR spectra is that the structuring of the visible part of the absorption spectra of these complexes is due to the presence of several electronic transitions and not to vibrational fine structure as was assumed in earlier work.

Supporting Information Available: Four tables describing results from DFT calculations on [(^{i}Pr-DAB)Pt(Ph)$_2$] and collective rR data of all complexes. This material is available free of charge via the Internet at http://pubs.acs.org.

Acknowledgment. This work was undertaken as part of the European collaborative COST project D14/0001/99. A.K. would like to thank Prof. D. J. Stufkens (UvA) for the opportunity to do research in his group and also for fruitful discussions, and Prof. W. Kaim (IAC, Universität Stuttgart) is acknowledged for financial support. We are also grateful for a loan of K_2PtCl_4 by Johnson Matthey (JM). S.Z. thanks also the Ministry of Education of the Czech Republic for the financial support (OC.D14.20).

IC025547O